Supporting Information:

The Ecology of Wildlife Disease Surveillance:

Demographic and prevalence fluctuations undermine surveillance

Laura Walton[1,2,3], Glenn Marion[1*], Ross S. Davidson[2], Piran C.L. White[3], Lesley A. Smith[2], Dolores Gavier-Widen[4], Lisa Yon[5], Duncan Hannant[5] and Michael R. Hutchings[2]

1. Biomathematics and Statistics Scotland, Edinburgh, United Kingdom
2. Disease Systems Team, SRUC, Edinburgh, United Kingdom
3. Environment Department, University of York, York, United Kingdom
4. Swedish University of Agricultural Sciences, Uppsala, Sweden
5. School of Veterinary Medicine and Science, University of Nottingham, United Kingdom

Appendix S1. Model implementation

Model implementation

The model is implemented as a set of coupled Stochastic Differential Equations, (SDEs) (see e.g. Mao 1997) and simulated using the Euler-Maruyama algorithm (e.g. see Higham 2001) which is essentially a generalisation of the Euler discretisation for Ordinary Differential Equations to SDEs. The model is also implemented (for simulation study 2) as a continuous-time discrete-state space Markov process, simulated using Gillespie's algorithm (Gillespie 1976). The Gillespie algorithm is an event-based method that makes use of the fact that in the underlying discrete state-space Markov process at any point in time the waiting time between events is exponential and parameterised by the total rate of all possible events i.e. the sum of all possible events. The Gillespie algorithm proceed from time t *by* drawing a waiting time τ from this distribution, advancing time to $t+\tau$, and then selects the nature of the event at random but weighted according to the relative rates of the possible events. The SDE implementation has been constructed so that it is the diffusion limit of the Gillespie implementation, ensuring that the results are consistent between the two implementations (see below). The Gillespie algorithm is computationally more intensive; by contrast, using SDEs is faster and therefore

facilitates both more accurate estimation of model statistics (i.e. a greater number of surveillance bouts can be run) and more extensive exploration of parameter space. However, the discrete nature of the state-space under the Gillespie algorithm is a more direct implementation of the model described in Table 1, and provides a more accurate representation of population dynamics especially for small populations.

Relationship between discrete and continuous (SDE) state-space model implementations.

In this appendix we describe the relationship between the continuous time discrete state-space Markov process and the stochastic differential equation (SDE) implementations of the model described in the main text.

Our starting point is the SI model described in Table 1 (main text) implemented as a continuous time discrete state-space Markov process in which the number of infected individuals $I(t)$ and total population size $N(t) = S(t)+I(t)$, are represented as integer variables. The Gillespie algorithm exploits the fact that the time between events is distributed exponentially with parameter $R(t)$ given by the sum of all the event rates in Table 1 and the probability that a given event occurs is given by the associated event rate divided by $R(t)$.

However, under this implementation one can also consider the expectation and variance-covariance of the change in the state-space variables $I(t)$ and $N(t)$ during a small time interval. For convenience denote the state of the system at time t by $X(t)=\{I(t),N(t)\}$. Then for example, conditional on the state of the system at time t, the expected change in the population size associated with birth events from time t to $t+\delta t$ is given by $E_B[\delta N(t)|X(t)] = rN(t)\,(1 - N(t)/k)\delta t$. Similarly, the variance in δN associated with birth events is $Var_B[\delta N(t)]= rN(t)\,(1 - N(t)/k)\delta t + O(\delta t^2)$, and henceforth we will assume δt is sufficiently small to ignore the higher order terms. In the model described in the main text (see Table 1 and surrounding text) all individuals are born susceptible and therefore birth does not affect the infective population size $I(t)$ i.e. $E_B[\delta I(t)|X(t)] = 0$, $Var_B[\delta I(t)]=0$, and $Cov_B[\delta I(t),\delta N(t)|X(t)]=0$. However, migration of infectives affects both $I(t)$ and $N(t)$ and to first order in δt we find that $E_{ml}[\delta N(t)|X(t)]= \gamma v \delta t$, $Var_{ml}[\delta N(t)]= \gamma v \delta t$, $E_{ml}[\delta I(t)|X(t)] = \gamma\ v\ \delta t$, $Var_{ml}[\delta I(t)]= \gamma\ v\ \delta t$ and $Cov_{ml}[\delta I(t),\delta N(t)|X(t)]= \gamma v \delta t$. The full set of first- and second-order statistics describing changes in the state-space associated with each event type are given (up to first order in δt) in Table S1.

Etype	Event	$E[\delta N\|X(t)]$	$E[\delta I\|X(t)]$	$Var[\delta N\|X(t)]$	$Var[I\|X(t)]$	$Cov[\delta N,\delta I\|X(t)]$
B	Birth	$rN(1-N/k)\delta t$	0	$rN(1-N/k)\delta t$	0	0
DS	Death of Susceptible	$-\mu S\delta t$	0	$\mu S\delta t$	0	0
DI	Death of Infected	$-\mu I\delta t$	$-\mu I\delta t$	$\mu I\delta t$	$\mu I\delta t$	$\mu I\delta t$
mS	Susceptible Immigration	$(1-\gamma)\nu\delta t$	0	$(1-\gamma)\nu\delta t$	0	0
mI	Infected Immigration	$\gamma\nu\delta t$	$\gamma\nu\delta t$	$\gamma\nu\delta t$	$\gamma\nu\delta t$	$\gamma\nu\delta t$
1ry	Primary Transmission	0	$\beta_0 S\delta t$	0	$\beta_0 S\delta t$	0
2ry	Secondary Transmission	0	$\beta IS\delta t$	0	$\beta_0 S\delta t$	0

Table S1: Expectations and variance-covariances in changes (during the time interval *t* to *t*+δt) to the state space {*I*(*t*),*N*(*t*)} associated with each event type in the discrete state-space model described in the main text (see Table 1). All such quantities are shown to first order in δt. Note: capture and release events are omitted since they affect neither *I*(*t*) or *N*(*t*).

We now show how to construct a continuous time, continuous state-space (diffusion) version of the model which is consistent with above implementation in that it preserves the means and variance-covariance statistics shown in Table S1. To do so we construct a set of stochastic differential equations (SDEs) which we later solve numerically in discrete time steps (e.g. see Higham 2001). The following Itô stochastic differential equations represent the change in the system state variables during an infinitesimally small time interval *dt*

$$dN(t) = \Big(f_{N,B}\big(X(t)\big) + f_{N,DS}\big(X(t)\big) + f_{N,DI}\big(X(t)\big) + f_{N,mS}\big(X(t)\big) + f_{N,mI}\big(X(t)\big) + f_{N,1ry}\big(X(t)\big) + f_{N,2ry}\big(X(t)\big)\Big)\,dt + g_{N,B}\big(X(t)\big)dB_B(t) + g_{N,DS}\big(X(t)\big)dB_{DS}(t) + g_{N,DI}\big(X(t)\big)dB_{DI}(t) + g_{N,mS}\big(X(t)\big)dB_{mS}(t) + g_{N,mI}\big(X(t)\big)dB_{mI}(t) + g_{N,1ry}\big(X(t)\big)dB_{1ry}(t) + g_{N,2ry}\big(X(t)\big)dB_{2ry}(t)$$

$$dI(t) = \Big(f_{I,B}\big(X(t)\big) + f_{I,DS}\big(X(t)\big) + f_{I,DI}\big(X(t)\big) + f_{I,mS}\big(X(t)\big) + f_{I,mI}\big(X(t)\big) + f_{I,1ry}\big(X(t)\big) + f_{I,2ry}\big(X(t)\big)\Big)\,dt$$

$$+ g_{I,B}\big(X(t)\big)dB_B(t) + g_{I,DS}\big(X(t)\big)dB_{DS}(t) + g_{I,DI}\big(X(t)\big)dB_{DI}(t)$$
$$+ g_{I,mS}\big(X(t)\big)dB_{mS}(t) + g_{I,mI}\big(X(t)\big)dB_{mI}(t)$$
$$+ g_{I,1ry}\big(X(t)\big)dB_{1ry}(t) + g_{I,2ry}\big(X(t)\big)dB_{2ry}(t)$$

Here the quantities $B_B(t)$, $B_{DS}(t)$, $B_{DI}(t)$, $B_{mS}(t)$, $B_{mI}(t)$, $B_{1ry}(t)$, $B_{2ry}(t)$ are independent Brownian motions corresponding to each of the seven event types and the correct interpretation of these equations requires consideration of associated stochastic intergrals (Mao, 1997). For small but finite *dt* the quantities $dB_B(t)$, $dB_{DS}(t)$, $dB_{DI}(t)$, $dB_{mS}(t)$, $dB_{mI}(t)$, $dB_{1ry}(t)$, $dB_{2ry}(t)$ can be interpreted as independent draws from a zero mean Gaussian with variance *dt* for each event type and each time point $0, dt, 2dt, \ldots, T \in (0,T)$. Thus e.g. $E[dB_B(t)]=0$, $E[dB_B(t)dB_B(t)]=0$ and $E[dB_B(t)dB_{DS}(t)]=0$. This discretisation is the basis for the numerical simulation of these SDEs used in this paper.

The so-called drift, $f_{N,B}(X(t))$, $f_{N,DS}(X(t))$, $f_{N,DI}(X(t))$, $f_{N,mS}(X(t))$, $f_{N,mI}(X(t))$, $f_{N,1ry}(X(t))$, $f_{N,2ry}(X(t))$ and diffusion, $g_{N,B}(X(t))$, $g_{N,DS}(X(t))$, $g_{N,DI}(X(t))$, $g_{N,mS}(X(t))$, $g_{N,mI}(X(t))$, $g_{N,1ry}(X(t))$, $g_{N,2ry}(X(t))$, terms representing changes in the variable $N(t)$ and the corresponding quantities representing changes in $I(t)$ are deterministic functions of the state-space $X(t)$ determined as follows.

Given the nature of the Brownian motions taking the expectation of the above equations yields

$$E[dN(t)|X(t)] = \Big(f_{N,B}\big(X(t)\big) + f_{N,DS}\big(X(t)\big) + f_{N,DI}\big(X(t)\big) + f_{N,mS}\big(X(t)\big) + f_{N,mI}\big(X(t)\big)$$
$$+ f_{N,1ry}\big(X(t)\big) + f_{N,2ry}\big(X(t)\big)\Big)\,dt$$
$$E[dI(t)|X(t)] = \Big(f_{I,B}\big(X(t)\big) + f_{I,DS}\big(X(t)\big) + f_{I,DI}\big(X(t)\big) + f_{I,mS}\big(X(t)\big) + f_{I,mI}\big(X(t)\big)$$
$$+ f_{I,1ry}\big(X(t)\big) + f_{I,2ry}\big(X(t)\big)\Big)\,dt$$

Which suggests that for each event type *Etype* $f_{N,Eype}(X(t))$ and $f_{I,Etype}(X(t))$ should be interpreted as the mean update shown in Table S1 for $N(t)$ and $I(t)$ respectively. For example, $f_{N,1ry}\big(X(t)\big)$ and $f_{N,2ry}\big(X(t)\big)$ are both zero since only birth, death and migration change the population size, i.e. neither primary nor secondary infection changes the population size.

The variance in the update for $N(t)$ is given by

$$\text{Var}[dN(t)|X(t)] = E[dN(t)^2|X(t)] - E[dN(t)|X(t)]^2$$

However, we have just shown that E[$dN(t)|X(t)$] is of order dt and therefore to first order in dt we can write

$$\text{Var}[dN(t)|X(t)] = E[dN(t)^2|X(t)] =$$
$$g_{N,B}\big(X(t)\big)^2 dt + g_{N,DS}\big(X(t)\big)^2 dt + g_{N,DI}\big(X(t)\big)^2 dt + g_{N,mS}\big(X(t)\big)^2 dt$$
$$+ g_{N,mI}\big(X(t)\big)^2 dt + g_{N,1ry}\big(X(t)\big)^2 dt + g_{N,2ry}\big(X(t)\big)^2 dt$$

and

$$\text{Var}[dI(t)|X(t)] = E[dI(t)^2|X(t)] =$$
$$g_{I,B}\big(X(t)\big)^2 dt + g_{I,DS}\big(X(t)\big)^2 dt + g_{I,DI}\big(X(t)\big)^2 dt + g_{I,mS}\big(X(t)\big)^2 dt$$
$$+ g_{I,mI}\big(X(t)\big)^2 dt + g_{I,1ry}\big(X(t)\big)^2 dt + g_{I,2ry}\big(X(t)\big)^2 dt$$

Here we have made use of the independent nature of the Brownian motions described above.

These last two equations therefore suggest that for each event type Etype, $g_{N,Etype}(X(t))^2$ and $g_{I,Etype}(X(t))^2$ should be interpreted as the variance in update shown in Table S1 for N(t) and I(t) respectively.

The above calculations are summarised in Table S2. Comparison with Table S1 allows the functional form for each drift and diffusion term to be identified.

Finally, the covariance

$$\text{Cov}[dN(t)dI(t)|X(t)] = E[dN(t)dI(t)|X(t)] - E[dN(t)|X(t)]E[dI(t)|X(t)]$$

to first order in dt is given by

$$\mathrm{Cov}[dN(t)dI(t)|X(t)] = E[dN(t)dI(t)|X(t)] =$$

$$+\ g_{N,DI}(X(t))g_{I,DI}(X(t))dt + \ g_{N,mI}(X(t))g_{I,mI}(X(t))dt$$

where we have shown only the non-zero terms. Comparison with the functional forms for the diffusion terms described above shows that this expression is consistent with the covariance terms shown in Table S1.

Etype	**E[dN|X(t)]**	**E[dI|X(t)]**	**Var[dN|X(t)]**	**Var[dI|X(t)]**	**Cov[dN,δI|X(t)]**
B	$f_{N,B}(X(t))dt$	$f_{I,B}(X(t))dt$	$g_{N,B}(X(t))^2dt$	$g_{I,B}(X(t))^2dt$	0
DS	$f_{N,DS}(X(t))dt$	$f_{I,DS}(X(t))dt$	$g_{N,DS}(X(t))^2dt$	$g_{I,DS}(X(t))^2dt$	0
DI	$f_{N,DI}(X(t))dt$	$f_{N,DI}(X(t))dt$	$g_{N,DI}(X(t))^2dt$	$g_{I,DI}(X(t))^2dt$	$g_{N,DI}(X(t))g_{I,DI}(X(t))dt$
mS	$f_{N,mS}(X(t))dt$	$f_{I,mS}(X(t))dt$	$g_{N,mS}(X(t))^2dt$	$g_{I,mS}(X(t))^2dt$	0
mI	$f_{N,mI}(X(t))dt$	$f_{I,mI}(X(t))dt$	$g_{N,mI}(X(t))^2dt$	$g_{I,mI}(X(t))^2dt$	$g_{N,mI}(X(t))g_{I,mI}(X(t))dt$
1ry	$f_{N,1ry}(X(t))dt$	$f_{I,1ry}(X(t))dt$	$g_{N,1ry}(X(t))^2dt$	$g_{I,1ry}(X(t))^2dt$	0
2ry	$f_{N,2ry}(X(t))$dt	$f_{I,2ry}(X(t))dt$	$g_{N,2ry}(X(t))^2dt$	$g_{I,2ry}(X(t))^2dt$	0

Table S2: Expectation and variance-covariances in changes (during the time interval *t* to *t*+*dt*) to the state space {*I*(*t*),*N*(*t*)} associated with each event type in the SDE model as described in Appendix S1. All such quantities are shown to first order in *dt*. Comparison with Table S1 enables both drift e.g. $f_{N,B}(X(t))$ and diffusion e.g. $g_{N,B}(X(t))$ functions to be identified. Note: capture and release events are omitted since they affect neither *I*(*t*) or *N*(*t*).

References

Higham, D. J. (2001) An Algorithmic Introduction to Numerical Simulation of Stochastic Differential Equations. *SIAM REVIEW* **43**(3), 525–546

Mao, X., (1997) *Stochastic Differential Equations and Applications*. Horwood, New York.

Appendix S2. Parameterisations used.

This section of the appendix describes in detail the parameter combinations used to produce the graphs in the main text. Values of the form: a,b,c,d etc refer to discrete values used for different lines shown on the Figures. Values of the form a;b;c refer to smallest value; largest value; step size describing the range of values (e.g. of the death rate) simulated to produce the Figures. Values of the form a – b refer to the range of values covered with a non-constant step size. All other parameters with single values are held constant in simulations.

Rate Name	Rate	Value
Secondary Transmission Rate	β	1.0, 0.1, 0.04, 0.01
Carrying Capacity	k	120
Growth Rate	r	0.5
Death Rate	μ	0.1;0.5;0.1
Immigration	ν	0.1
Infected Immigration Proportion	γ	0.1
Primary Transmission Rate	β_0	0
Susceptible Active Capture	α	0.1
Infected Active Capture	α	0.1
Sample Target	m	10.0

Table S3: Parameter values are shown for Figure 1 in the main text which demonstrates the effect of the death rate and transmission rate on the bias and variance of the prevalence estimate as well as the effect of the death rate on the population size and variance. 10^6 surveillance bouts are run of each combination and terminate when the sample target is reached, i.e. there is no time limit imposed. These parameters were implemented using the SDE version of the model.

Rate Name	Rate	Value
Secondary Transmission Rate	β	1.0, 0.1
Carrying Capacity	k	120
Growth Rate	r	0.5
Death Rate	μ	0.4, 0.43
Immigration	ν	0.1
Infected Immigration Proportion	γ	0.1
Primary Transmission Rate	β_0	0
Susceptible Active Capture	α	0 - 10
Infected Active Capture	α	0 - 10
Sample Target	m	10.0

Table S4: Parameter values are shown for Figure 2 in the main text which demonstrates the effect of the capture rate on the bias and variance of the prevalence estimate. 10^6 surveillance bouts are run of each combination and terminate when the sample target is reached, i.e. there is no time limit imposed. These parameters were implemented using the SDE version of the model.

Rate Name	Rate	Value
Secondary Transmission Rate	β	1.0, 0.1
Carrying Capacity	k	120
Growth Rate	r	0.5
Death Rate	μ	0.4, 0.43
Immigration	ν	0.1
Infected Immigration Proportion	γ	0.1
Primary Transmission Rate	β_0	0
Susceptible Active Capture	α	0.1
Infected Active Capture	α	0.1
Sample Target	m	1 - 10000

Table S5: Parameter values are shown for Figure 2 in the main text which demonstrates the effect of the sample size on the bias and variance of the prevalence estimate. 10^6 surveillance bouts are run of each combination and terminate when the sample target is reached, i.e. there is no time limit imposed. These parameters were implemented using the SDE version of the model.

Rate Name	Rate	Value
Secondary Transmission Rate	β	1.0, 0.1, 0.04, 0.01
Carrying Capacity	k	120
Growth Rate	r	0.5
Death Rate	μ	0.1;0.5;0.01
Immigration	ν	0.1
Infected Immigration Proportion	γ	0.1
Primary Transmission Rate	β_0	0
Susceptible Active Capture	α	10, 1.0, 0.1, 0.01
Infected Active Capture	A	10, 1.0, 0.1, 0.01
Sample Target	M	10

Table S6: Parameter values are shown for Figure 3 in the main text which demonstrates the effect of the death rate and transmission rate, as well as the sample size and capture rate, on the probability of detecting disease. 10^6 surveillance bouts are run of each combination and terminate when the sample target is reached, i.e. there is no time limit imposed. These parameters were implemented using the SDE version of the model.

Rate Name	Rate	Value
Secondary Transmission Rate	B	0.01,0.05,0.09,0.2,0.6, 1.0,2.0,5.0
Carrying Capacity	K	1;36.0;3.5
Growth Rate	R	0.5;23;2.5
Death Rate	μ	0.25;14.0;1.25
Immigration	N	1.0
Infected Immigration Proportion	Γ	0.01
Primary Transmission Rate	β_0	0.01
Susceptible Active Capture	A	0.5
Infected Active Capture	A	0.5
Sample Target	M	10.0, 20.0

Table S7: Parameter values are shown for Figure 4 in the main text which demonstrates the effect of the transmission, death rate, birth rate, carrying capacity, as well as the sample size, on the probability of detecting disease. 1000 simulations were run per parameter combination with a time limit of 45. If the simulation did not reach the sample target within the time limit, the run is discarded and not used in the statistical calculations. If out of 1000 realisations a parameter combination ceases to reach the sample target at least 15 times, that parameter combination is discarded totally as the results are deemed to be unreliable. Increasing the time limit bears little to no effect on the amount simulations which reach the target sample, so the precise value of the time limit does not affect the results obtained from the model. These parameters were implemented using the Gillespie version of the model.

Appendix S3. Additional scenarios.

This appendix shows results for a set of scenarios complimentary to those in the main text. It is shown that the effects described in the main text are robust to three factors: population size; mode of secondary transmission and sample size.

Population size

The simulations in the main text are based on relatively small populations where fluctuations are driven only by demographic stochasticity. Here we simulate disease dynamics and surveillance in a population driven by environmental stochasticity (see below for details). This enables consideration of fluctuations in a much larger population since demographic fluctuations reduce with population size whereas environmental fluctuations do not. We show that in a population larger by a factor of approximately 10-100 compared with that described in the main text (Fig. 1 and Fig 3.), and using a sample size that is 10 times larger, the effects described are if anything greater. When compared with calculations based on assuming constant prevalence we see that the probability of detecting disease is reduced and estimates of prevalence are both biased and less precise (see Fig. S1 and Fig. S2).

The model used is as described in the main text but here the death rate is subjected to a correlated random walk based on a mean reverting Ornstein-Uhlenbeck process. With finite time step dt this is represented as

$$\mu(t+dt) = \mu(t) + \left(\mu_0 - \mu(t)\right) b_\mu \, dt + \sigma_\mu \, dB_\mu(t)$$

where $dB_\mu(dt), dB_\mu(2dt), \ldots$ are independent identically distributed Gaussian random variables with zero mean and variance dt. The above equation is integrated along with the equations described in Appendix S1. After a burn-in period the equilibrium dynamics of this equation fluctuate around the mean μ_0. The parameter b_μ controls the correlation in time of $\mu(t)$ and in the long run the variance in $\mu(t)$ is given by $\sigma_\mu / 2\, b_\mu$. The resulting fluctuations in mortality rate represent a range of environmental conditions from harsh to mild which drive fluctuations in the population size. The results shown in Fig. S1 and Fig. S2 are based on this model and the parameter values shown in Table S8. They show qualitatively the same effects seen in Fig. 1 and Fig. 3 in the main text.

Rate Name	Rate	Value
Secondary Transmission Rate	B	1.0, 0.1, 0.04, 0.01
Carrying Capacity	K	6000
Growth Rate	R	1.0
Death Rate	μ_0	0.025;1.0;0.025
Immigration	N	0.1
Infected Immigration Proportion	Γ	0.1
Primary Transmission Rate	β_0	0
Susceptible Active Capture	A	0.001
Infected Active Capture	A	0.001
Sample Target	M	100.0
	b_μ	0.4
	σ_μ	0.5

Table S8: Parameter values are shown for Figures S1 and S2. 10^6 surveillance bouts are run of each combination and terminate when the sample target is reached, i.e. there is no time limit imposed. These parameters were implemented using the SDE version of the model incorporating the stochastic variation in the death rate described above.

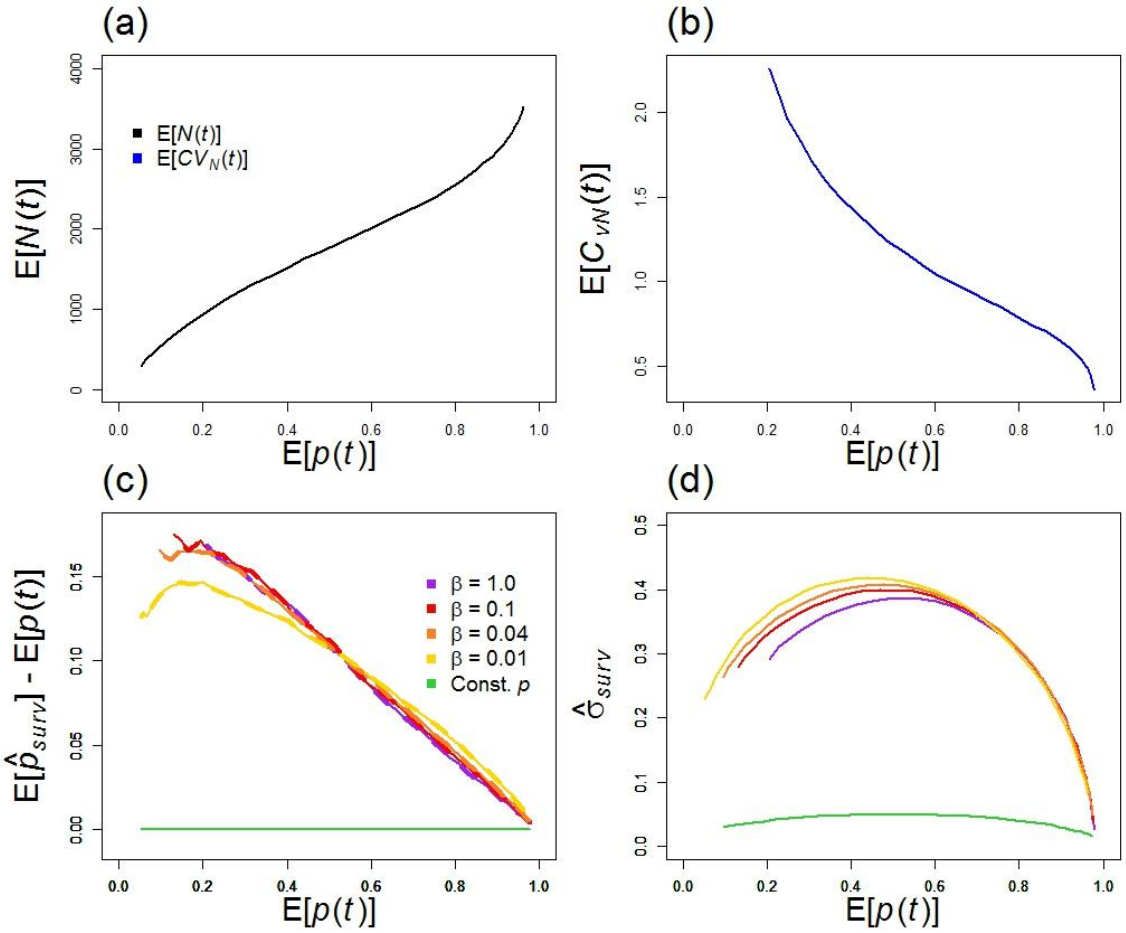

Figure S1: This figure is the counterpart to Fig. 1 in the main text but for the large population simulations with fluctuating death rate described above. The typical population sizes range from around 500-3000 and the sample size used is 100.

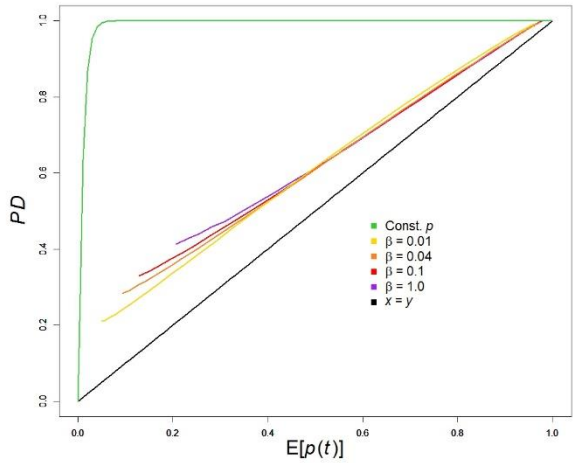

Figure S2 Probability of disease detection. This plot is the counterpart to Fig 3c in the main text but for the large population described above.

Frequency dependent transmission

The scenario simulated here is identical to that shown in Figs 1 and 3 in the main text except that here disease transmission is frequency dependent such that secondary infections occur at rate

$$\tilde{\beta}\frac{S(t)\,I(t)}{N(t)}$$

Recall that the total population size at time t is $N(t)$ and is made up of $S(t)$ susceptible and $I(t)$ invectives. Contrasting the above formulation with the density dependent transmission rate $\beta S(t)\,I(t)$ it is clear that to ensure comparable rates of transmission we require $\tilde{\beta} \approx \beta N$. Therefore to ensure comparability between the simulations of frequency and density dependent transmission the contact rate $\tilde{\beta}$ is given by

$$\tilde{\beta} = \beta\, K \frac{(r-\mu)}{r}$$

where β is the density dependent transmission rate and $K\,(r-\mu)/r$ is the equilibrium population size derived from the deterministic version of the model.

The results shown in Fig. S3 and Fig S4 show that the effects described in the main text are just as evident in the case of frequency dependent transmission as they are for density dependent transmission.

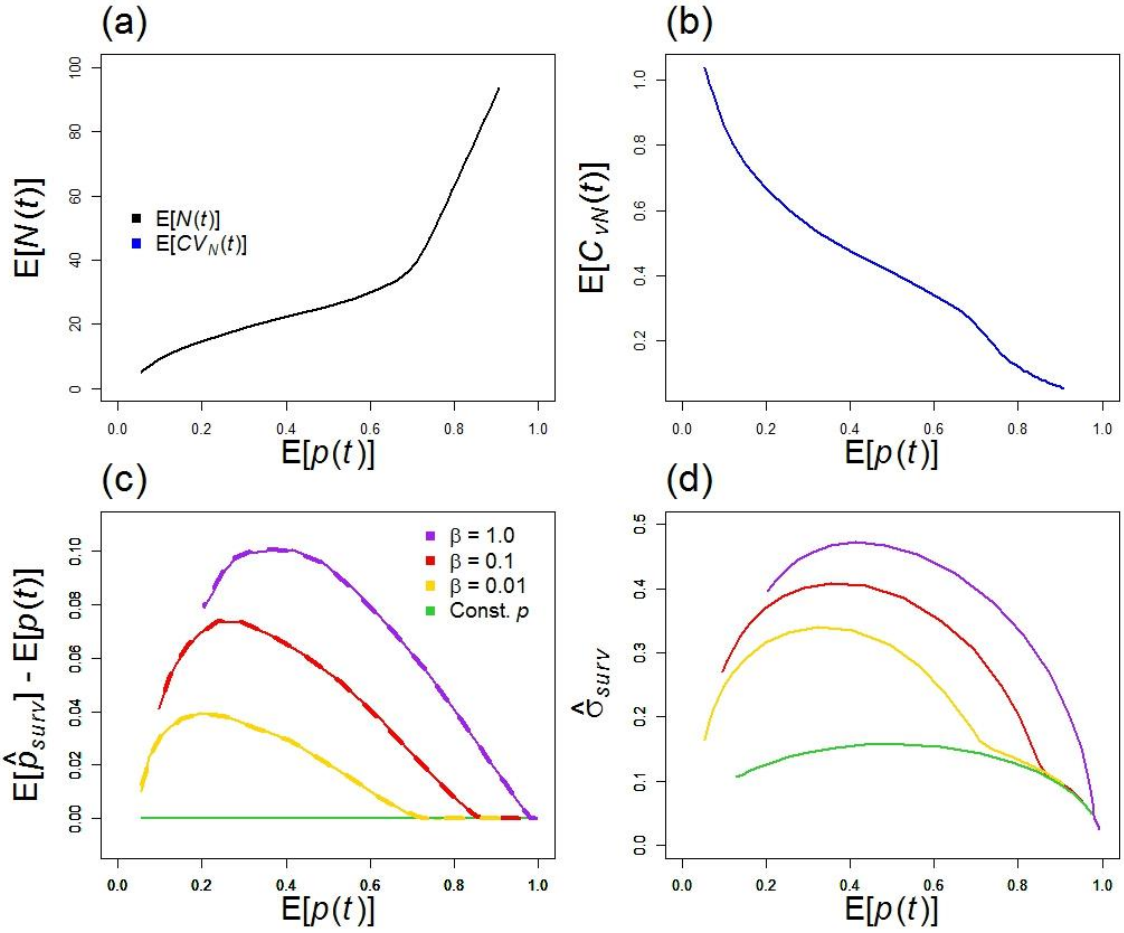

Figure S3: Equivalent to Fig 1 in the main text but for the frequency dependent transmission described above described above.

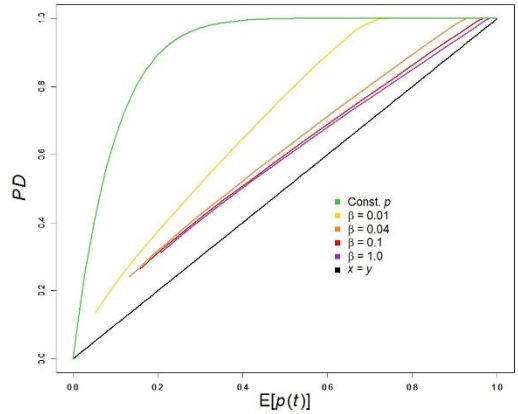

Figure S4 Probability of disease detection. This plot is the counterpart to Fig 3c in the main text but for the frequency dependent transmission described above described above.

Sample size:

Here we show results from a scenario identical to that shown in Figures 1 and 3 of the main text except that the sample size is increased from 10 to 20 and 50. In this scenario the population is typically between 10 and 40 individuals so although these sample sizes may seem low they represent a large fraction of the population. The figures below demonstrate that sample size has little effect on the degradation in the performance of surveillance. Thus these results support the conclusion drawn from Fig. 2 in the main text.

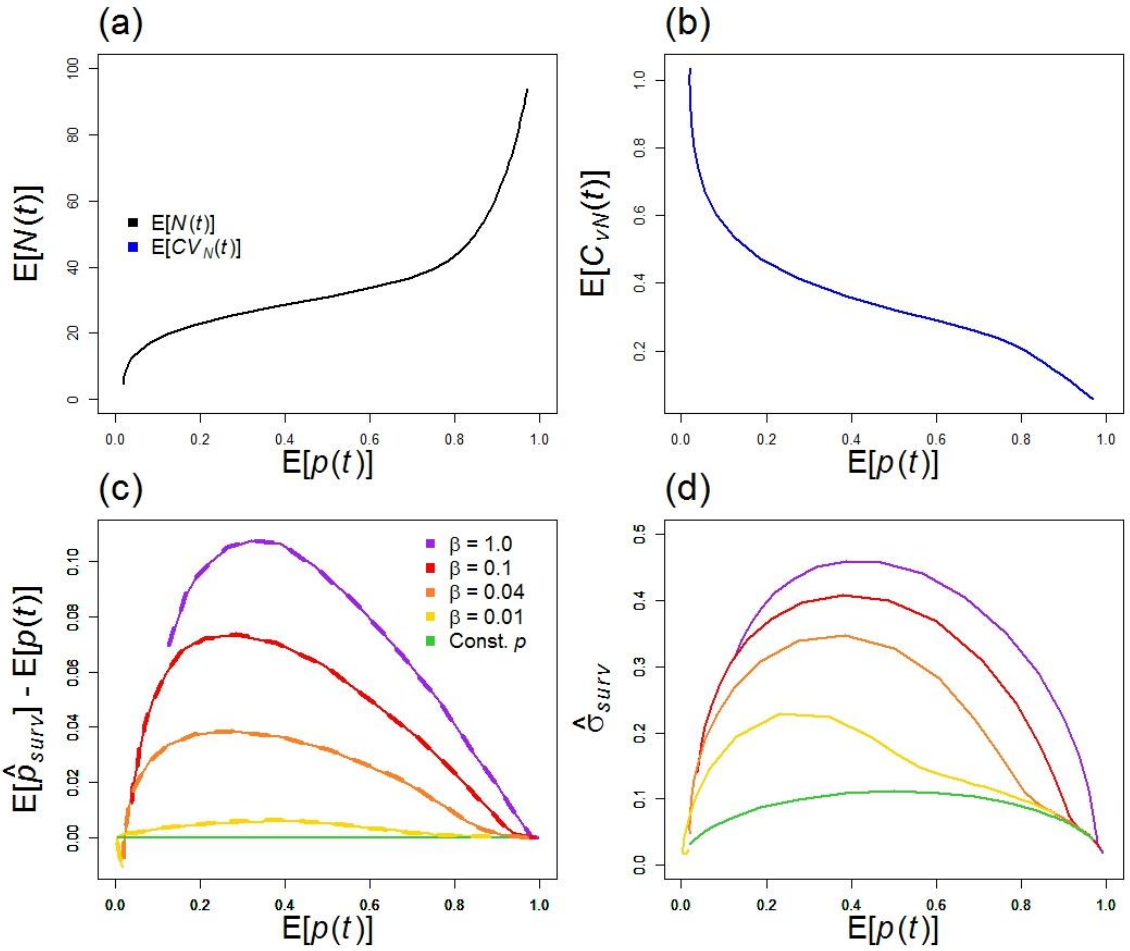

Figure S1: This figure depicts the scenario shown in Figure 1 of the main text but with sample size 20.

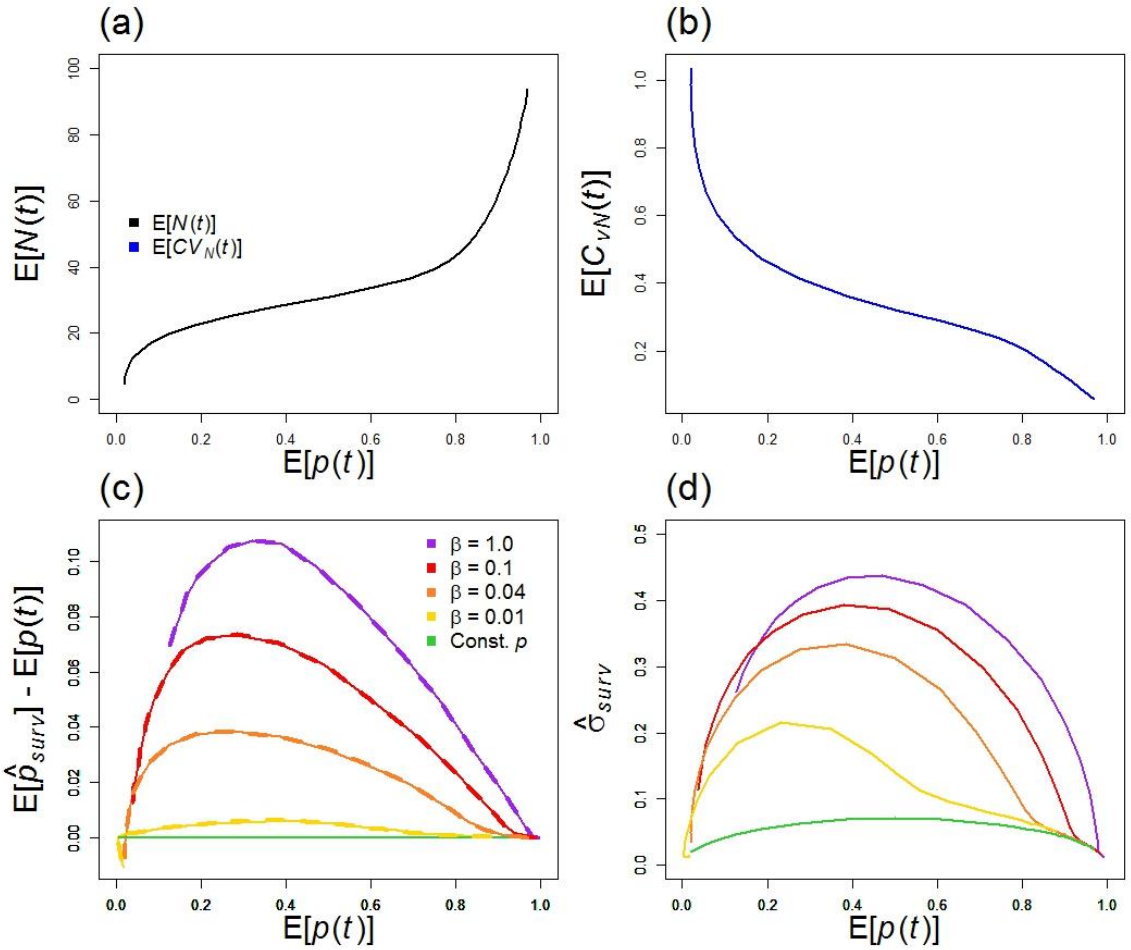

Figure S2: This figure depicts the scenarios shown in Figure 1 of the main text but with sample size 50.

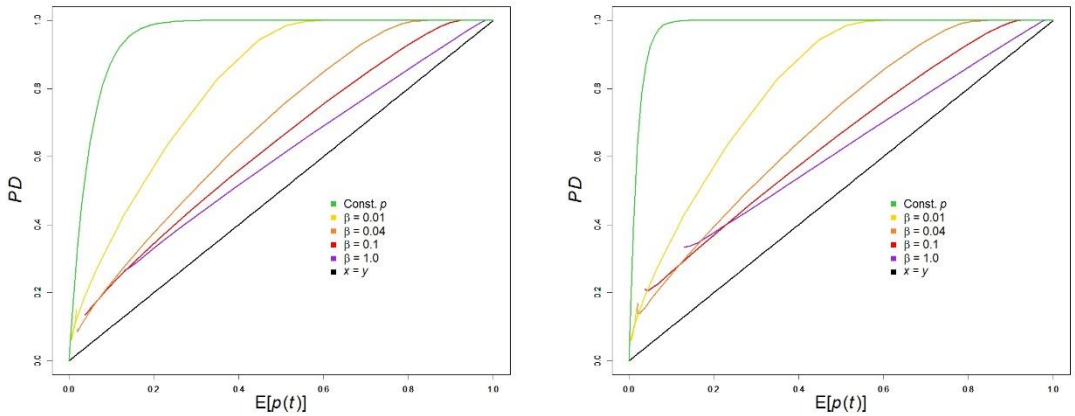

Figure S3: Probability of detection. This plot is the counterpart to Fig 3c in the main text but for increased sample sizes. The plot on the right shows sample size 20 and that the right 50 whereas Fig 3c is based on sample size 10.

Appendix S4. Analysis of disease detection probability

In many cases the primary goal of wildlife disease surveillance is detection of disease rather than quantification of prevalence. This is true, for example, for emerging or re-emerging disease, where detection is a precursor to further action, which would include heightened surveillance. If prevalence is assumed constant and equal to the long term average prevalence $\mathrm{E}[p]$ of the wildlife disease system, then the probability that disease is detected in a sample of size m is given by:

$$PD^{Bin} = f(\mathrm{E}[p], m) = 1 - (1 - \mathrm{E}[p])^m$$

This formula, based on simple binomial arguments, and variants that also assume constant prevalence, are the standard basis for sample size calculations (see e.g. Fosgate 2009). However, if prevalence fluctuates PD^{Bin} is a misleading estimate of the probability of detection.

In real systems, prevalence varies with time; therefore, when conducting surveillance, the prevalence values will vary at the times when each of the m samples are collected. Nonetheless, for simplicity here we assume that the prevalence during a given surveillance bout (i.e. the collection of m consecutive samples) is constant, and denoted p. Fig. 3a (see main text) compares the probability of detection measured from simulations with two approximations. The first approximation accounts for fluctuations both within and between surveillance bouts and the second only that between surveillance bouts. These results indicate that accounting only for fluctuations between surveillance bouts is an accurate approximation. Therefore, the expected probability of detection for sample size m is defined as

$$PD = \mathrm{E}[f(p, m)] = \mathrm{E}[1 - (1 - p)^m]$$

where the expectation is over the between bout prevalence distribution $\mathrm{P}(p)$ which accounts only for prevalence fluctuations between surveillance bouts. For a single sample $m = 1$, the above equation for PD reduces to a linear form, so that $PD = PD^{Bin} = E[p]$. However, if $m > 1$, then the equation for PD is non-linear, and therefore $PD \neq PD^{Bin}$.

To illustrate this, we Taylor expanded PD by assuming that the difference between the bout prevalence (p) and the long term average prevalence is small i.e. $p = E[p] + \Delta p$. Then, noting that $E[\Delta p] = 0$ and $var[p] = E[\Delta p^2]$ and ignoring terms containing higher powers of Δp, this yields

$$PD \cong PD^{Bin} + \frac{1}{2} var[p] \left. \frac{\partial^2 f(p,m)}{\partial p^2} \right|_{p=E[p]}$$

This suggests (to leading order in the expansion) that the true probability oction will be lower than PD^{Bin}, since the second derivative $\partial^2 f(p,m)/\partial p^2 = -m(m-1)(1-p)^{m-2}$ is negative for sample size $m > 1$ and $p = E[p]$. In addition, the size of this deviation depends on the sample size and the variance in prevalence. Although these conclusions are broadly correct, when compared with simulation results, the above Taylor expansion does not provide an accurate approximation of the probability of detection. However, analytic progress can be made, with the following alternative approach. The approximation $(1-p)^m \approx e^{-pm}$ holds for m large (and is already accurate even for $m = 10$) and enables us to write the probability of detection as:

$$PD = 1 - \mathrm{E}_p[(1-p)^m] \cong 1 - \mathrm{E}[e^{-pm}] = 1 - M_p(m)$$

where $M_p(m) \equiv E[e^{-pm}]$ is the moment generating function associated with the between bout prevalence distribution $\mathrm{P}(p)$. This suggests that if we could parameterise a suitable distribution to approximate $\mathrm{P}(p)$ then we could use the corresponding moment generating function to calculate the probability of detection.

Fig. 3a (main text) suggests that a moment-generating function approximation (see last equation above) based on the actual distribution of prevalence between surveillance bouts would be an accurate approximation. Fig. 3b illustrates this approximation using an assumed gamma distribution, parameterised with the mean and variance of $\mathrm{P}(p)$. Although the gamma approximation is not completely successful, it does provide a more accurate prediction of PD than PD^{Bin}. This could be used to improve sample size calculations in situations where simulation is not possible, but information about prevalence fluctuations is available. Moreover, the results of Fig. 3a show that such approximations could be improved by assuming a more accurate representation of the prevalence distribution $\mathrm{P}(p)$.